Available online at www.sciencedirect.com
SCIENCE DIRECT®
Inorganica Chimica Acta 357 (2004) 3920–3926
Inorganica Chimica Acta
www.elsevier.com/locate/ica

Catalytic size control of multiwalled carbon nanotube diameter in xylene chemical vapor deposition process

Nitin Chopra [a], Bruce Hinds [a,b,*]

[a] Department of Chemical and Materials Engineering, University of Kentucky, 177 Anderson Tower, Lexington, KY 40506-0046, USA
[b] Department of Chemistry, University of Kentucky, 177 Anderson Tower, Lexington, KY 40506-0046, USA

Received 31 March 2004; accepted 7 August 2004
Available online 23 September 2004

Abstract

Multiwalled carbon nanotubes (CNT) of diameters of 10–40 nm are synthesized on Fe and Co coated nm-scale catalyst support in a xylene chemical vapor deposition (CVD) process without the need for ferrocene iron source. Silica (~40 nm diameter) and nanocrystalline Au (~10 nm) are coated with a monolayer of amine, sulfonate, or thiol termination to ensure monolayer Fe loading, reduce Fe surface migration and reduce agglomeration of catalyst support particles during dispersion. Coordination with surface functionalization did not noticeably hinder Fe surface diffusion nor hinder catalytic activity of CNT formation. CNT diameters of ~40 nm were seen for most chemical treatments. Functionalization of substrate (SiO_2/Si) surface with carboxylic termination aided in the dispersion of amine functionalized silica nanoparticles. Another approach to limit catalytic support to nm-scale dimensions was to deposit a thin film of Co (5–25 nm thick) in a multilayer structure that after etching left a nm-scale Co line at the edge of the pattern. In the ferrocene CVD process, CNT diameters down to 10 nm are controlled directly by the catalytic metal film thickness.

Keywords: Carbon nanotubes; Thin films; Catalysis

1. Introduction

Numerous advances in electronics [1–3] sensors [4], and nanomechanical systems [5] are possible with the use of carbon nanotubes (CNT) due to ballistic electron conduction and extreme tensile strength. Critical for the practical realization of applications is the control of CNT diameter and its placement in an integrated device. Due to the long length of tubes, it is possible to use micron scale lithography processes for manipulation of CNTs into an integrated device, yet have nm-scale line width or tube diameter. One particularly novel application is to use CNTs as a shadow mask in a line-of-site deposition process resulting in nm-scale line-widths [6]. The line widths can be further reduced by controlling evaporate incident angle with simple slits [7]. Discrete CNTs spanning photolithographically defined posts has been reported [8,9] and is largely made possible since the numerous CNTs that do not bridge between posts fall to the side. However this approach requires further diameter control for lithography applications. The catalytic route to carbon filaments and nanofibers has long been studied [10,11], with the filament diameter being determined by the size of the nm-scale catalyst particle [12–14]. Gaseous carbon sources form a super-saturated carbide eutectic that ejects graphitic sheets at the relatively high temperature of 900 °C. The catalyst can be metal particle [15] or metal salt coatings on catalyst support [16,17]. Surface migration and coarsening give a relatively wide distribution of size, thus it is desired to

* Corresponding author. Tel.: +1 859 266 7037; fax: +1 859 323 1929.
E-mail address: bjhinds@engr.uky.edu (B. Hinds).

0020-1693/$ - see front matter © 2004 Elsevier B.V. All rights reserved.
doi:10.1016/j.ica.2004.08.022

have well dispersed and uniform nanocrystal particles [18,19]. However, it remains a significant challenge to place only a few nanoparticles in predefined locations without agglomeration or coarsening [20].

Coarsening and migration effects are reduced at lower temperature, thus a xylene/ferrocene based chemical vapor deposition (CVD) method to grow multiwalled CNTs at temperatures of 600–700 °C is appealing. In this process ferrocene decomposes to continuously supply an iron source for forming catalyst nanoparticles from which CNTs emanate. This process can grow CNTs at high densities with noteworthy alignment [21,22]. The diameter of the resultant CNT is a complicated system that involves the surface free energy of catalyst and substrate, surface migration, and ferrocene decomposition rates. By controlling temperature, xylene and ferrocene feed rate it is possible to determine multiwalled CNT diameters in the range of 30–100 nm with 10% dispersion. By using the etched edged of a thin film multilayer structure ($Si/SiO_2/Si$) with a 10–60 nm thick SiO_2 layer, we demonstrate that CNT diameter can be controlled (±3 nm standard deviation) [23]. In this example ferrocene forms nc-Fe only on the exposed SiO_2 catalyst support, with nc-Fe diameter set by layer thickness. The use of an exposed edge of a multilayer film structure is a novel method to set a nanotube's diameter and is a readily scalable process. However, the $Si/SiO_2/Si$ multilayer growth process requires careful removal of native silicon dioxide by HF acid, which complicates processing. Thus, it is of interest to examine the xylene CNT growth process without ferrocene. Specifically, can pre-placed nc-Fe or chemical precursors direct CNT growth with diameter control? Of particular interest is whether the dimensions of nm-scale catalyst support coated with catalyst can determine the CNT diameter. The xylene CVD system has an advantage of lower growth temperatures 600–700 °C. Reported here is the growth of CNTs in a ferrocene-free CVD process by both self-assembly of Fe coordinating ligands to nm-scale catalyst support particles as well as on the edge of a cut catalytic metallic thin film multilayer structure. Diameters of CNTs as small as 10 nm are determined by the thickness of the metallic film interlayer.

2. Experimental methods

2.1. Materials used

Colloidal gold nanoparticles (10 nm diameter) and colloidal silica nanoparticles (45 nm diameter) were purchased from Aldrich. 1,6-Hexanedithiol, 96% ($HS(CH_2)_6SH$), 2-mercapto ethane sulfonic acid, sodium salt, 98% ($HSCH_2CH_2SO_3Na$), 4-aminobenzenethiol ($H_2NC_6H_4SH$), 3-aminopropyltriethoxysilane (APTES), 99% ($H_2N(CH_2)_3Si(OC_2H_5)_3$). 4-(Triethoxysilyl) butyronitrile (TBN), and 98% ($(C_2H_5O)_3Si(CH_2)_3CN$) were also obtained from Aldrich. Ferric chloride and $FeCl_3$ bought from Mallinckrodt; ethanol and C_2H_5OH were from Aaper alcohol and chemical company; DI water (18 MΩ cm) was obtained using Barnstead DI water supply; sulfuric acid H_2SO_4 were from Spectrum; xylene was purchased from Fisher Scientific; and silicon wafer (p-type, ⟨1 0 0⟩) was purchased from International Wafer Service.

2.2. Modification of silica colloidal nanoparticles with silane monolayer coated with iron catalyst

0.5 ml colloidal silica nanoparticles of diameter 10 nm were added to a 5 ml of 2 mM ethanolic solution of APTES. The solution was left for an overnight reaction at room temperature and after which the solution was centrifuged for 30 min at 3200 rpm. The supernatant obtained was almost transparent and was removed leaving behind milky white residue. The residue was washed 4–5 times with ethanol and DI water and finally dispersed in ethanol. An aliquot of the above colloidal dispersion in ethanol was added to 2 ml of 21 mM $FeCl_3$ in DI water. The mixture was stirred for 30 min followed by centrifuging at 3200 rpm and 30 min and the supernatant was removed to exclude excess $FeCl_3$. The residue was washed 4–5 times with DI water and stored finally in ethanol.

2.3. Modification of gold colloidal nanoparticles with thiol monolayer coated with iron catalyst

1 ml of colloidal gold nanoparticles of diameter 10 nm were added to 5 ml of 10 mM ethanolic solution of 1,6-hexanedithiol. After an overnight reaction at room temperature, the solution was centrifuged at 3200 rpm for 30 min. The supernatant was removed and the residue was washed 4–5 times in ethanol and DI water and was finally stored in ethanol. A few ml of the above solution was added to 2 ml of 21 mM $FeCl_3$ in DI water. The mixture was stirred for 30 min followed by centrifuging at 3200 rpm and 30 min and the supernatant was removed to exclude excess $FeCl_3$. The residue was washed 4–5 times with DI water and was stored finally in ethanol. Similarly, various other thiol compounds like 2-mercaptoethanesulfonic acid, sodium salt and 4-aminobenzenethiol were self-assembled onto gold nanoparticles and coated with iron catalyst by using $FeCl_3$ solution.

2.4. Preparation of silicon wafer with carboxylic acid terminated surface

RCA cleaned Si wafer was immersed in 100 ml of 10.6 mM solution of 4-(triethoxysilyl) butyronitrile (TBN) for an overnight reaction. After the reaction, a

nitrile terminated Si wafer was rinsed with water to remove any unbound molecules. The nitrile terminated wafer was immersed in 5 M H_2SO_4 and heated at an average temperature of 120 °C for 5 min and then rinsed with water for 20 s and dried in air. This step was an acid hydrolysis reaction to convert nitrile groups into carboxylic acid.

2.5. Preparation of colloidal assembly onto carboxylic acid modified silicon substrate

A carboxylic acid modified silicon substrate is immersed for 5–10 min in an ethanolic solution of Fe coated silane modified silica colloidal particles (or Fe coated thiol modified gold colloidal particles) followed by rinsing with DI water for 15–20 s. The substrate was allowed to dry in air and then transferred to tube furnace for CNT growth via chemical vapor deposition.

2.6. CNT growth via xylene chemical vapor deposition

CNTs were grown on the samples by pyrolysis of xylene under Ar/H_2 atmosphere in a cleaned tubular furnace used for ferrocene/xylene multiwalled CNT growth [22]. The quartz tube (3 in. diameter) was purged with Argon (flow rate: 675 ml/min) for 5 min. The furnace was heated to 700 °C and while maintaining the injector temperature at 220 °C, H_2 was introduced in the quartz tube at rate of 75 ml/min. Pure xylene was injected into the reactor through the syringe injector at the rate of 30 ml/min for a brief duration of 2 min 4 s and then the xylene flow was reduced to 1 ml/min and continued for 2 h. The liquid xylene exiting the capillary tube was immediately volatilized and swept into the reaction zone of the furnace at 700 °C by the flow of argon with 36.2% hydrogen. After 2 h the furnace was allowed to cool down to room temperature in flowing argon.

2.7. CNT growth on exposed edge of cobalt in SiO_2/Co/SiO_2 thin film multilayer structure

An RCA cleaned silicon wafer was first coated with 114 nm thick SiO_2 in an e-beam evaporator (Thermionics laboratory Hayward, CA) at starting pressure of $\sim 10^{-6}$ Torr. Cobalt films of three different thicknesses (5, 10, and 25 nm, respectively) were sputter coated (DC Sputtering, AJA International) thermally oxidized Si substrates. The cobalt layer on each sample was finally coated with another 135 nm thick SiO_2 layer in an e beam evaporator. The samples were patterned with positive photo resist (Shipley 1813) through photolithography (using Karlsuss MJB3 mask aligner) and followed by an ion beam etching (E.A Fischione Instruments Inc.) at a beam angle of 45°, current value of 2 mA, and 5 kV voltage. The etching time was approximately 2 h 30 min and the etch rate estimated for SiO_2 was 120 nm/min. The ion beam etching process facilitated formation of an exposed edge of SiO_2/Co/SiO_2 thin film multilayer structure analogous to the multilayer structure reported in our previous work [23]. The samples were immersed in boiling acetone for 2 min and 30 s to remove the photo resist on the thin film multilayer structure. Finally, CNTs were grown on the three samples following the same CVD method as previously described [22], except without ferrocene source and a growth duration of 30 min.

2.8. Characterization

The microstructure of resultant CNT growth and diameters were characterized by Hitachi S900 field emission electron source SEM at 3 keV with 2–5 nm resolution.

3. Results and discussion

Growth of multiwalled CNTs is observed in a xylene-based CVD process without the use of ferrocene iron source. Fig. 1 shows typical CNT growth on chemically modified silica support coated with $FeCl_3$. Table 1 shows a close correlation of the CNT diameter to the

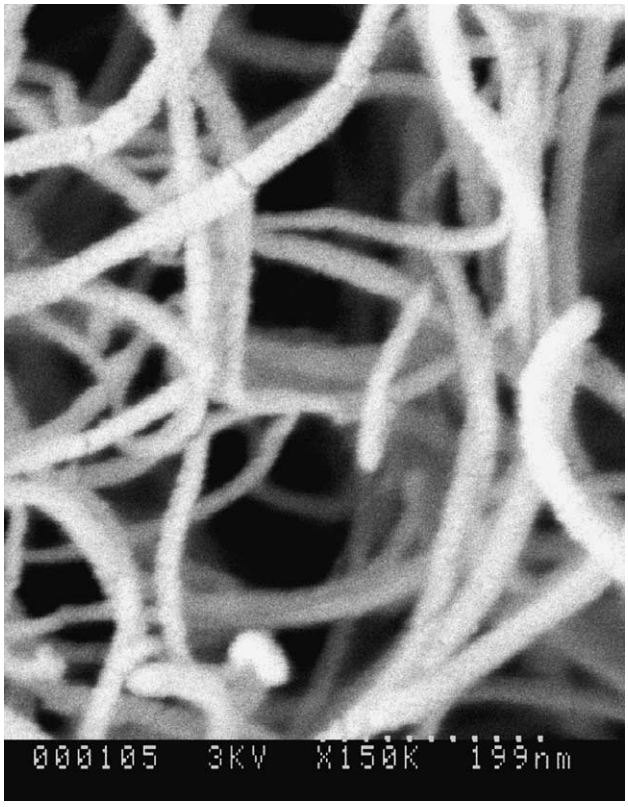

Fig. 1. CNTs resulting from xylene CVD process on chemically modified silica nanoparticles at 700 °C. Silica nanoparticles were self-assembled with 3-aminopropyltriethoxysilane (APTES) and then coated with $FeCl_3$.

Table 1
Comparison of CNT diameters with catalyst support size

Sample	Average diameter (nm)	Median diameter (nm)	Average standard deviation (nm)
Nanoparticles of silica on a Si wafer (surface of nanoparticles is modified by APTES and coated with $FeCl_3$)	49.16	40.00	23.78
Carbon nanotubes grown on silica nanoparticles modified with APTES and coated with iron (labeled as sample number 8 and 10, respectively, in Fig. 2).	43.41	43.64	5.86

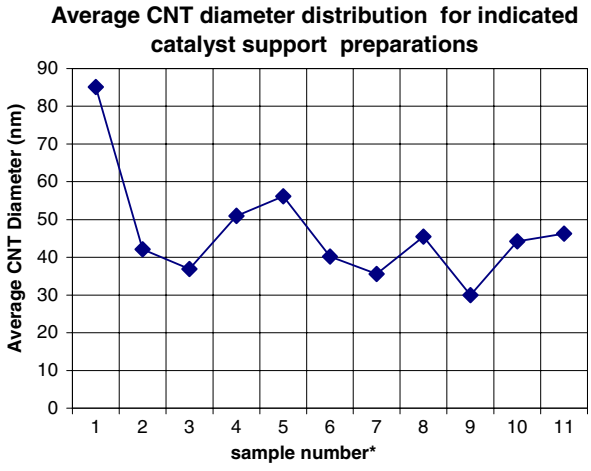

*** Sample Number**

1 – Au (colloidal) surface modified with Mercapto ethane sulphonic acid and coated with Iron. (dispersed in hexane solvent)
2 – Au (colloidal) surface modified with 1, 6 hexane dithiol and coated with Iron. (dispersed in EtOH)
3 – Au (colloidal) surface modified with Mercapto ethane sulphonic acid and coated with Iron. (dispersed in EtOH)
4 – Au (colloidal) surface modified with 4-Amino thiophenol and coated with Iron. (washed in hexane and then dispersed in EtOH)
5 - SiO_2 (colloidal) surface modified with APTES and coated with Iron. (dispersed in hexane solvent)
6 – SiO_2 (powder) modified with APTES and Iron. (washed in CH_2Cl_2 and then dispersed in EtOH)
7 – SiO_2 (colloidal) surface modified with APTES and coated with Iron. (dispersed in EtOH)
8 – SiO_2 (colloidal) surface modified with APTES and coated with Iron. (washed in hexane and then dispersed in EtOH)
9 - SiO_2 (colloidal) surface modified with APTES and coated with Iron. (dispersed in EtOH)
10 - SiO_2 (colloidal) surface modified with APTES and coated with Iron. (dipersed in EtOH)
11 - SiO_2 (colloidal) surface modified with APTES and coated with Iron. (dispersed in hexane)

Fig. 2. Average CNT diameter observed after CNT growth from silica and gold nanoparticles which were modified and then coated with iron catalyst.

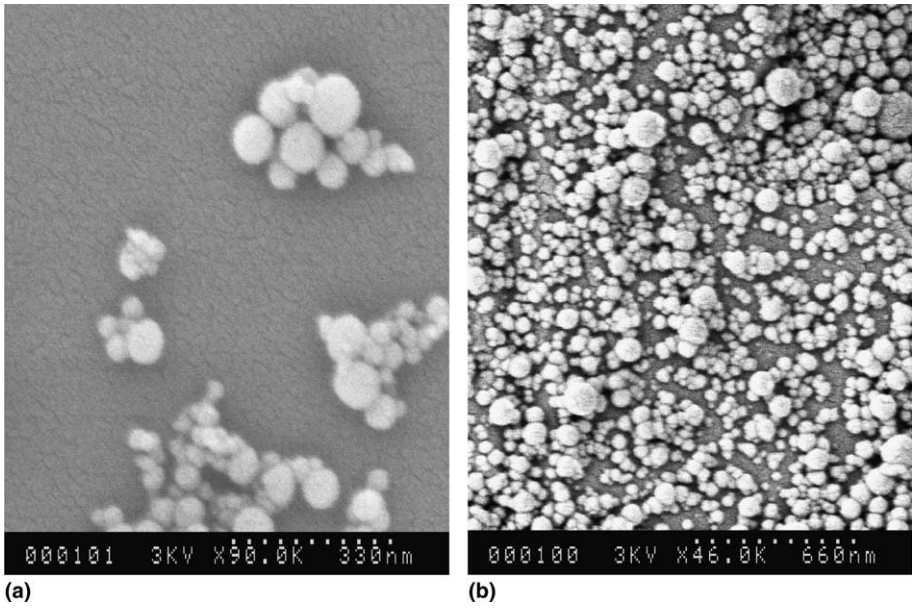

Fig. 3. (a) Agglomerated particles of SiO_2 on wafer after storage in hexane. (b) Nanoparticles of SiO_2 modified with 3-amino propyl triethoxysilane (APTES) and coated with $FeCl_3$. Wafer is treated with COOH terminated SAM that enhances binding of catalyst particles to the substrate, reducing agglomeration and increasing areal density.

diameter of silica particles, however the standard deviation of silica particle diameters is significantly different. This suggests that there is significant Fe surface migration to an equilibrium Fe nanocrystal size. The formation of larger nc-Fe particles would be further enhanced by agglomeration of catalyst support particles during their dispersion onto SiO_2/Si substrate. Thus it is of interest to hinder Fe surface diffusion by chemical coordination to surface functional groups or reduce catalyst support particle agglomeration. Fig. 2 summarizes CNT diameter function of catalyst treatment during xylene CVD process. In general CNT diameters remained near 40 nm suggesting a similar nanocrystal nucleation/growth limit that is commonly seen in ferrocene/xylene CVD growth conditions. The first four samples (of Fig. 2) used 10 nm diameter Au nanocrystals coated with thiol-based coordination compounds (amine, sulfonate, and thiol end groups). The CNT diameter was clearly not determined by the individual nanoparticle diameter indicating Fe migration and or agglomeration of nc-Au particles. Amine surface chemistry appears to have little effect on Fe migration during CVD process. It is quite likely that the surface alkanes are consumed during the CNT growth process. Importantly thiol groups do not poison Fe catalyst, allowing well established Au/thiol self-assembly chemistry to determine the location of catalyst particles. Also the use of chemical coordination of Fe to the nanoparticles ensures a fixed monolayer dosing of catalyst.

Fig. 3 also shows the significance of nanoparticle agglomeration during dispersion of nanoparticles. Dispersion in non-polar solvents such as hexane increase agglomeration, however polar solvents such as H_2O can dissolve weakly coordinated $FeCl_3$. EtOH was found to be a good balance, though there is typically clustering at the edge of the drop during drying process.

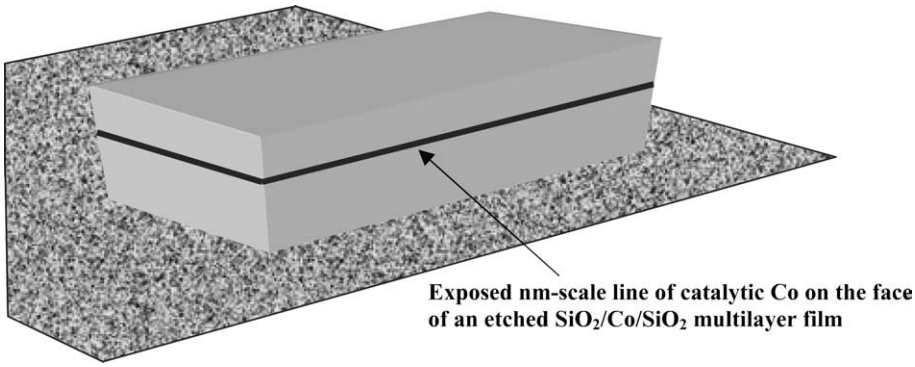

Fig. 4. Schematic of nm-scale line width (dark colored) from etched edge of a SiO_2/Co/SiO_2 thin film multilayer structure. The thickness of cobalt middle layer defines the diameter of CNTs selectively growing out from it.

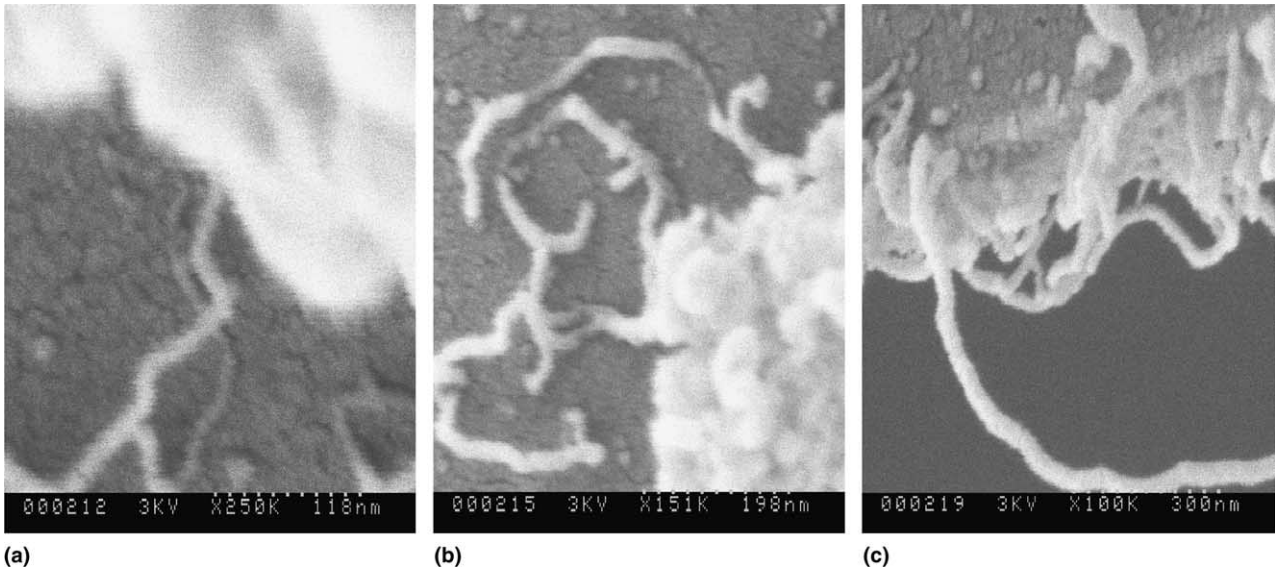

Fig. 5. SEM images of CNTs grown from exposed edge of Co thin film in SiO_2/Co/SiO_2 thin film multilayer structure. (a) Co thickness ~5 nm, (b) Co thickness ~10 nm, (c) Co thickness ~25 nm.

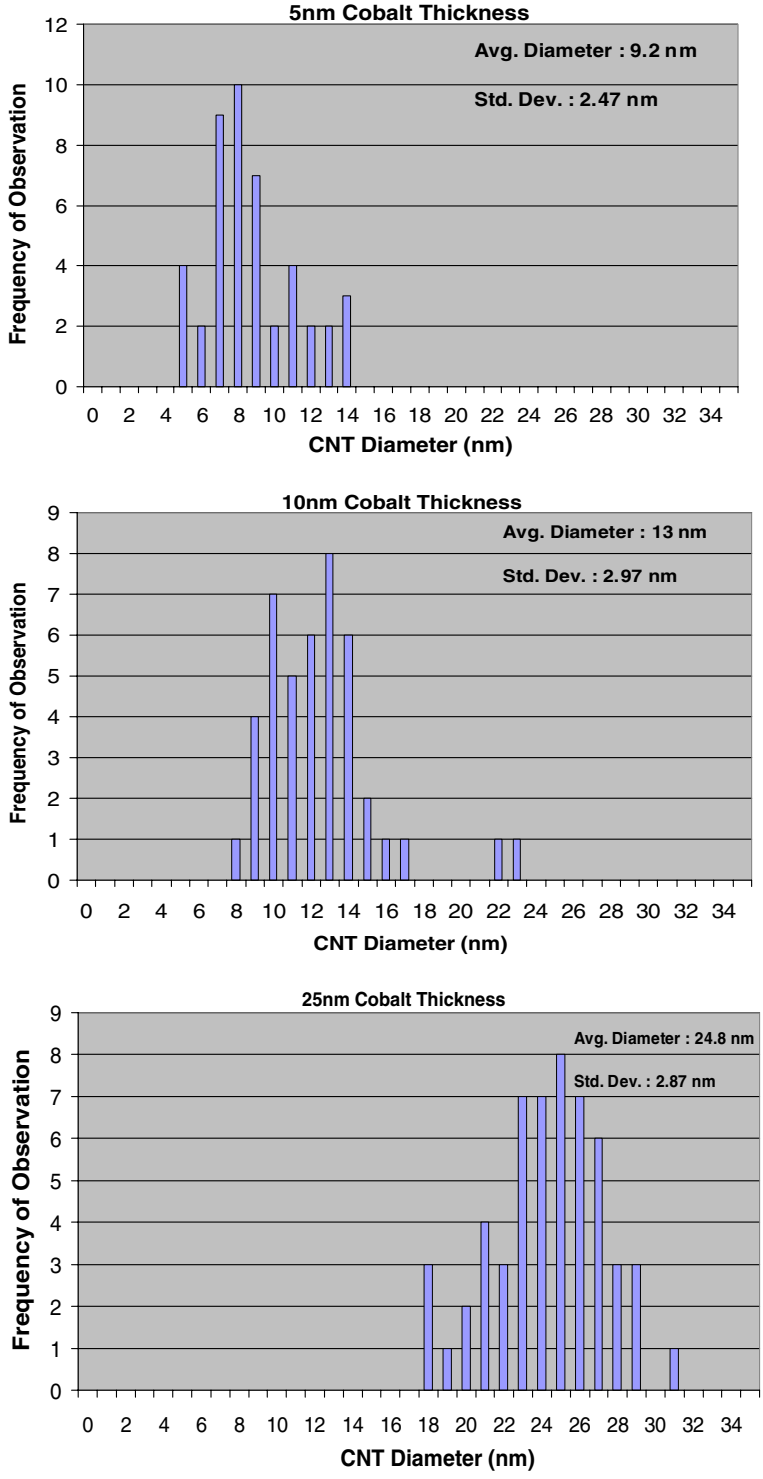

Fig. 6. Histogram of observed CNT diameter as a function of Co film thickness after xylene CVD growth at 700 °C.

Treating the SiO_2/Si wafer surface with COOH terminated ligands allows coordination with amine terminated nc-silica particles. Fig. 3(b) shows that this approach resulted in a decrease in agglomeration of support particles as well as an increase in surface coverage ($\sim 2 \times 10^8$ cm^{-2}). CNT diameters of near 40 nm are seen after the CVD process.

Another method to avoid the effects of agglomeration is to directly pattern metalic catalyst. A novel approach to pattern catalyst with nm-scale line width, is to use the

edge of a metallic thin film multilayer structure as diagrammed in Fig. 4. The width of the catalytic line in principle could determine the diameter of the CNTs catalytically grown from the edges. The approach to control CNT diameter is similar to that previously reported where a thin line of SiO_2 was a catalyst support for ferrocene decomposition into nc-Fe and subsequent growth of CNTs. There is a report of using an edge of a catalytic metal multilayer structure (50–100 nm thick) to grow CNTs, however no diameter control was seen due to the relatively large thickness [24]. Fig. 5 shows SEM micrographs of CNTs grown from the edge of Co thin films in xylene CVD growth. Observed CNTs diameters of 9.2 (2.5) nm, 13 (3.0) nm and 24.8 (2.9) nm were seen for 5, 10, and 25 nm thick Co films, respectively (see Fig. 6). Similar results were seen with Fe catalyst, but CNT lengths were markedly shorter. The ion milling processing step was performed at a 45° angle which would leave an exposed metal line width of 1.414 times the film thickness. At lower film thickness (5 and 10 nm) CNT diameter is consistent with that angle (i.e., 7 and 14 nm), while for thicker films (25 nm) the resulting CNT diameter is close to the actual film thickness. Further experiments in etch angle, film thickness, and capping layer material are required to understand the mechanism of nanocrystal/droplet formation at the step edge during the Co/C eutectic formation.

4. Conclusions

The relatively low temperature (700 °C) xylene CVD process is robust and does not require continuous Fe feed with ferrocene vapors. Fe coated nanocrystals are an appropriate support with observable diameter control to 40 nm, which is commonly seen in xylene/ferrocene CVD growth of CNTs. However difficulties in Fe migration and agglomeration of particles during dispersion remain a significant challenge that is only moderately influenced by chemical surface modification and dispersion control. Exposed edges of a catalytic metal thin film in multilayer structure can be used to precisely control CNT diameter down to 10 nm. This multilayer can be readily incorporated onto photolithographically defined posts allowing for integration into electronic or micro electro mechanical systems (MEMS). In principle these CNTs can be grown to span posts [8,9] which can used for wiring or lithographic processes [6]. Importantly for nanowires suspended above the substrate as shadow mask, the incident angle of line-of-site evaporation requires wire diameters of ~10 nm to cast 1–2 nm wide line shadows [7], This system of using thin catalytic thin films to laterally grow CNTs of controlled diameter is promising for such an application.

Acknowledgements

The authors thank Padmakar Kichambare and Rodney Andrews at the Center for Applied Energy Research (University of Kentucky) for use of their xylene CVD system and the Center for MicroMagnetic Electronic Devices (CMMED) provided equipment for thin film fabrication. The authors thank the NSF-MERSEC Advanced Carbon Materials Center (DMR-9809686), Kentucky RCTF as well as sponsorship by the Air Force Office of Scientific Research (DEPSCoR program) under agreement number F49620-02-1-0225.

References

[1] A. Bachtold, P. Hadley, T. Nakanishi, C. Dekker, Science 294 (2001) 1317.
[2] K. Tsukagoshi, B.W. Alphenaar, H. Ago, Nature 401 (1999) 572.
[3] K. Liu, P. Avouris, R. Martel, W.K. Hsu, Phys. Rev. B 6316 (2001), art. no. 161404.
[4] H. Chang, J.D. Lee, S.M. Lee, Y.H. Lee, Appl. Phys. Lett. 79 (2001) 3863.
[5] P.A. Williams, S.J. Papadakis, M.R. Falvo, A.M. Patel, M. Sinclair, A. Seeger, A. Helser, R.M. Taylor, S. Washburn, R. Superfine, Appl. Phys. Lett. 80 (2002) 2574.
[6] J. Lefebvre, M. Radosavljevic, A.T. Johnson, Appl. Phys. Lett. 76 (2000) 3828.
[7] N. Chopra, R. Andrews, W. Xu, L. DeLong, B.J. Hinds, Mat. Res. Soc. Symp. Proc. EXS-2 (2004) M5.4.1.
[8] A.M. Cassell, N.R. Franklin, T.W. Tombler, E.M. Chan, J. Han, H.J. Dai, J. Am. Chem. Soc. 121 (1999) 7975.
[9] N.R. Franklin, H.J. Dai, Adv. Mater. 12 (2000) 890.
[10] N.M. Rodriguez, J. Mater. Res. 8 (1993) 3233.
[11] R.T.K. Baker, M.A. Barber, R.J. Waite, P.S. Harris, F.S. Feates, J. Catal. 26 (1972) 51.
[12] S.B. Sinnott, R. Andrews, D. Qian, A.M. Rao, Z. Mao, E.C. Dickey, F. Derbyshire, Chem. Phys. Lett. 315 (1999) 25.
[13] C.L. Cheung, A. Kurtz, H. Park, C.M. Lieber, Chemistry B 106 (2002) 2429.
[14] E.F. Kukovitsky, S.G. L'Vov, N.A. Sainov, Chem. Phys. Lett. 317 (2000) 65.
[15] G.W. Ho, A.T.S. Wee, J. Lin, W.C. Tjiu, Thin Solid Films 388 (2001) 73.
[16] K. Hernadi, A. Fonseca, J.B. Nagy, D. Bernaerts, A. Fudala, A.A. Lucas, Zeolites 17 (1996) 416.
[17] K. Hernadi, A. Fonseca, P. Piedigrosso, M. Delvaux, J.B. Nagy, D. Bernaerts, J. Riga, Catal. Lett. 48 (1997) 229.
[18] H. Ago, T. Komatsu, S. Ohshima, Y. Kuriki, M. Yumura, Appl. Phys. Lett. 77 (2000) 79.
[19] Y. Li, J. Liu, Y.Q. Wang, Z.L. Wang, Chem. Mater. 13 (2001) 1008.
[20] O. Jost, A.A. Gorbunov, J. Moller, W. Pompe, A. Graff, R. Friedlein, X. Liu, M.S. Golden, J. Fink, Chem. Phys. Lett. 339 (2001) 297.
[21] R. Sen, A. Govindaraj, C.N.R. Rao, Chem. Phys. Lett. 267 (1997) 276.
[22] R. Andrews, D. Jacques, A.M. Rao, F. Derbyshire, D. Qian, X. Fan, E.C. Dickey, J. Chen, Chem. Phys. Lett. 303 (1999) 467.
[23] N. Chopra, P.D. Kichambare, R. Andrews, B.J. Hinds, Nano Lett. 2 (2002) 1177.
[24] Y.S. Han, J.K. Shin, S.T. Kim, J. Appl. Phys. 90 (2001) 5731.